Knockdown of Musashi-1 enhances chemotherapeutic sensitivity and apoptosis in Group 3/4 medulloblastomas cells

Pablo Shimaoka Chagas (pablochagas@usp.br)
Ribeirão Preto Medical School

Luciana Chain Veronez
Ribeirão Preto Medical School

Graziella Ribeiro de Sousa
Ribeirão Preto Medical School

Gustavo Alencastro Veiga Cruzeiro
Harvard Medical School - Dana-Farber Cancer Institute

Carolina Alves Pereira Corrêa
Ribeirão Preto Medical School

Fabiano Pinto Saggioro
Ribeirão Preto Medical School

Rosane Gomes de Paula Queiroz
Ribeirão Preto Medical School

Suely Kazue Nagahashi Marie
University of Sao Paulo

Silvia Regina Brandalise
Boldrini's Children Center

Izilda Aparecida Cardinalli
Boldrini's Children Center

José Andres Yunes
Boldrini's Children Center

Carlos Gilberto Carlotti Júnior
University of Sao Paulo

Hélio Rubens Machado
Ribeirão Preto Medical School

Marcelo Volpon Santos
Ribeirão Preto Medical School

Carlos Alberto Scrideli
Ribeirão Preto Medical School

Luiz Gonzaga Tone

Ribeirão Preto Medical School

Elvis Terci Valera

Ribeirão Preto Medical School

Research Article

Keywords: Grp3-MB, Grp4-MBs, RNA Binding-protein, Musashi-1

Posted Date: July 6th, 2022

DOI: https://doi.org/10.21203/rs.3.rs-1800310/v1

Abstract

Groups (Grp) 3 and 4 are aggressive molecular subgroups of medulloblastoma (MB), with high rates of leptomeningeal dissemination. To date, there is still a paucity of biomarkers for these subtypes of MBs. The RNA-binding protein Musashi-1 (*MSI1*) is a neural stem cell marker, characterized as a gene translation regulator and associated with high oncogenicity in several human cancers. In this study, we investigated the clinical significance and biological functions of *MSI1* in Grp3/Grp4-MBs. First, we assessed the expression profile of *MSI1* in 59 primary MB samples (15-WNT, 18-SHH, 9-Grp3, 17-Grp4 subgroups) by qRT-PCR. *MSI1* mRNA expression levels were also validated in an additional public dataset of MBs (GSE85217). The ROC curve was used to validate the diagnostic standards of *MSI1* expression. Cell cycle, cell viability, and apoptosis were evaluated in D283 Med cell-line (Grp3/Grp4/MBs) after shRNA-mediated knockdown of *MSI1* plus cisplatin treatment. We identified an overexpression of *MSI1* with a high accuracy to discriminate Grp3/Grp4-MBs from non- Grp3/Grp4-MBs. In addition, *MSI1* knockdown promoted cell cycle interruption in the G1/S transition and, consequently, decreased the number of cells in the G2/M phase, repressed cell proliferation and sensitized D283 Med cells to cisplatin treatment by enhancing cell apoptosis. The results of the present study are the first to demonstrate that *MSI1* may play a role as biomarker for Grp3/Grp4-MBs. In addition, *MSI1* knockdown combined with cisplatin may offer a potential strategy to be further explored in Grp3/Grp4-MBs.

Introduction

Medulloblastoma (MB, World Health Organization grade 4) is the most common malignant brain tumor in the pediatric population [1]. MBs originate in the cerebellum and are classified into four different molecular subgroups: Wingless signaling activated (WNT), Sonic Hedgehog (SHH), Groups 3 (Grp3-MBs) and 4 (Grp4-MBs) [1, 2]. Grp3 accounts for 25% of all MB cases, representing the deadliest of all molecular subgroups, with a 5-year overall survival (OS) ranging from 42 to 66%, depending on Grp3 subtypes (alpha, beta, or gamma)[3]. On the other hand, although accounting for around 40% of MBs cases, Grp4-MBs are still poorly biologically characterized with an OS of around 70% (intermediate prognosis). Intriguingly, both subgroups have a high propensity to metastasize [4-6]. Currently, the treatment options for MBs are based on multimodal strategies that include maximal safe resection, chemotherapy and radiotherapy [4]. However, surviving patients often suffer severe treatment-related side effects, including permanent cognitive and motor disabilities, particularly infants and children of pre-scholar age [6, 7]. In this context, it is of note the scantiness of effective targeted-therapies for Grp3/Grp4-MBs that could provide better overall survival, aligned with an improvement in patients' life quality. In fact, this lack of new actionable biomarkers depicts a challenge in the daily clinical practice due to the limited understanding of tumorigenesis and the inconclusive molecular stratification for Grp3/Grp4-MBs [1, 4].

Musashi-1 (*MSI1)* is an evolutionarily highly-conserved gene and member of the RNA-binding proteins (RBP) family, that was first identified in *Drosophila sp*. in 1994. Interestingly, this group of proteins received this name in honor to Miyamoto Musashi, a great swordsman of the Eastern culture [8]. *MSI1* is

crucial in the initiation of the development of the central nervous system (CNS) and is vastly expressed in neural progenitor cells of vertebrates, being characterized as neuronal stem cell (SC) marker [9-11]. *MSI1* acts through its direct interaction with the 3'-UTR (3' untranslated region) in several mRNA targets in a post-transcriptional level, inducing the increase or silencing the expression of these genes. For this reason, *MSI1* is recognized as a translational regulator of cell fate, and maintenance of the stem cell state [12, 13]. Dysregulations in *MSI1* expression can lead to cellular dysfunctions promoting tissue instability, as well as tumorigenesis [14]. Additionally, *MSI1* have been reported to regulate cell cycle, chemoresistance, proliferation and cell death in several tumors, including tumors of the CNS such as gliomas, glioblastomas and astrocytomas. Thus, in recent years, the role of *MSI1* in cancer has gained increasing interest [15-17].

Herein, we identified an overexpression of *MSI1* in Grp3/Grp4-MBs in a Brazilian cohort and in an independent dataset (GSE85217) of pediatric MBs. Next, the overexpression of MSI1 in Grp3/Grp4-MBs tumor samples were confirmed by immunohistochemistry. Besides, we also observed a significant role of *MSI1* expression in the discrimination between Grp3/Grp4-MBs from non-Grp3/Grp4-MBs. knockdown of *MSI1* by short-hairpin (sh) RNA in D283 Med cell-line (a Grp3/Grp4-MB cell-line) promoted cell cycle interruption in the G1/S transition and, consequently, decreased the number of cells in the G2/M phase, repressed cell growth and sensitized these cells to cisplatin treatment by enhancing cell apoptosis. Overall, our study provides for the first time, new insights of *MSI1* as potential target involved in Grp3/Grp4-MBs carcinogenesis.

Materials And Methods

Case Series / RNA extraction and cDNA synthesis

MSI1 mRNA levels were evaluated in a total of 59 pediatric patients (0-19 years) diagnosed with MBs in three Brazilian institutions that were previously classified as WNT (n=15), SHH (n=18), Grp3 (n=9), and Grp4 (n=17) [18], and in five non-neoplastic cerebellum, serving as controls. Total RNA was extracted from pediatric MB tissues and cell-lines using Trizol reagent (Invitrogen Inc, Carlsbad, USA) or AllPrep DNA/RNA/Protein Mini kit (QIAGEN, Hilden, Germany), following the manufacturers' specifications. RNA concentrations were determined by using the ND-1000 Spectrophotometer device (NanoDrop 1000 Technologies, Wilmington, DE, USA). The reverse transcription reaction for the synthesis of complementary DNA strand (cDNA) was performed using 500ng of total RNA and the High Capacity kit (Applied Biosystems, Foster City, CA, USA) according to the manufacturer's instructions. Additionally, expression data of an independent cohort of pediatric MBs (GSE85217, n=629) was downloaded from R2 Platform (Analysis and Visualization Platform – http://r2.amc.nl) [2] and used to validate *MSI1* expression levels between the different molecular subgroups of MBs.

Cell lines and culture conditions

The pediatric MB cell lines D283 Med and USP-13-MED 4 [19, 20] (Grp3/4-MBs), and the Human Embryonic Kidney 293 cell (HEK93T) were used in this study. D283 Med (ATCC HTB-185) and HEK-293

(ATCC CRL-1573) cells were obtained from the American Type Culture Collection, and the USP 13-MED cell line was kindly provided by Prof. Dr. Oswaldo Keith Okamoto - Biosciences Institute of the University of São Paulo. The cell lines authentications were performed to validate the Short Tandem Repeat (STR) prolife. All cells were maintained in DMEM/F12 medium (Gibco™, Thermo Fisher®, Carlsbad, CA, USA), supplemented with 10% FBS, 100U/ml penicillin, 100 µg/ml streptomycin and kept in a humid atmosphere containing 5% CO_2 at 37ºC.

Quantitative real-time PCR (qRT-PCR)

Relative mRNA expression levels were measured by quantitative PCR using TaqMan Gene Expression Assays (Applied Biosystems, Foster City, CA, USA- *MSI1* Hs01045894_m1) in 59 pediatric MB samples, and in D283 Med and USP-13-MED cell lines. The reactions were performed on QuantStudio™ 12k Flex system (Applied Biosystems, Foster City, CA, USA) using two internal controls: *GUSB* (Beta Glucuronidase) (Hs4333767F_m1) and *HPRT* (hypoxanthine guanine phosphoribosyl transferase) (Hs4310809E_m1). The data were analyzed using the $2^{-\Delta\Delta CT}$ method and non-neoplastic cerebellum samples were used as calibrators [21].

Immunohistochemistry (IHC)

IHC staining was performed on formalin-fixed paraffin-embedded (FPFE) tissue sections (4 µm) of eight MB samples (WNT n=2; SHH n=1; Grp3 n=3 and Grp4 n=2) using the detection system EnVision™ polymer (Dako, Glostrup, Denmark), following the manufacturers' recommendations. The antigen retrieval was carried out using citrate buffer (pH 6.0). The slides were incubated with anti-MSI1 antibody (dilution 1:70 cat. no. #5663, Cell Signaling Technology, Danvers, MA). Cerebral cortex was used as positive control [22]. The immunostaining was analyzed by a savvy neuropathologist, considering as positive cells those with cytoplasmic and/or nuclear staining for MSI1. Positive cells were scored according to the percentage of stained cells as following: Score (+) %, percentage of MSI1 positive tumor cells. + (< 25%), ++ (< 25-50%), +++ (< 50-75%) and ++++ (< 75-100%). Intensity of immunostaining (immunoreactivity) in tumor cells: Low (+), Strong (+ +). Representative cases were captured at ×40 magnification using Nikon ECLIPSE 80i.

Western blot (WB)

The wild type and transduced cells lines were lysed on ice in lysis buffer containing freshly added protease inhibitor cocktail (Roche Diagnostics, Branchburg, NJ, USA). Protein extracts (50µg) were size-fractionated by SDS-PAGE and proteins were immunoblotted with anti-MSI1 (dilution 1:1000, cat. no. #5663, Cell Signaling Technology, Danvers, MA). Anti-glyceraldehyde 3-phosphate dehydrogenase (GAPDH). All antibodies were diluted according to manufacturer's instructions and HRP-conjugated goat anti-rabbit (Santa Cruz Biotechnology, Santa Cruz, CA) was used as a secondary antibody. The results were visualized using an enhanced chemiluminescence detection system (Bio-Rad Laboratories, Inc.),

and the relative quantification of protein expression was determined using ImageJ® software (National Institutes of Health).

Immunofluorescence

For immunofluorescence staining, D283 Med and USP-13-MED cells were grown on glass coverslips and then fixed with 4% paraformaldehyde in PBS 1X for 15 minutes. After fixation, cells were permeabilized with 0.3% Triton X-100 at room temperature, washed with PBS 1X, and incubated with a blocking buffer (2% bovine serum albumin) for two hours. Samples were then incubated with primary antibody (1:500, Anti-Musashi-1 (D46A8) Rabbit mAb #5663, Cell Signaling Technology, Danvers, MA) in blocking buffer at 4^{o}C overnight. Finally, cells were washed three times with PBS 1X and then stained with Alexa Fluor 647 anti-rabbit secondary antibodies (1:2500) diluted in blocking buffer containing Alexa Fluor™ 488 Phalloidin – ThermoFisher (1:40) for 1 hour, followed by three washes in PBS 1X. Coverslips were mounted in ProLong Gold Mounting Medium containing the nuclear stain 4',6-diamidino2-phenylindole (DAPI) (Vectashield, Vector Laboratories, Burlingame, CA, EUA). Images were obtained using a laser scanning confocal microscope Leica DM2500 (LeicaBiosystems, Wetzlar, Germany) and the software LAS (Leica Biosystems, Wetzlar, Germany). Negative controls included incubation with secondary antibodies alone.

Lentivirus-mediated short hairpin RNA (shRNA) knockdown of gene expression

Silencing of *MSI1* was performed using two shRNA vectors (pLV[shRNA]-EGFP:T2A:Bsd-U6>hMSI1[shRNA#1] and pLV[shRNA]-EGFP:T2A:Bsd-U6>hMSI1[shRNA#2]), and their respective control (pLV[shRNA]-EGFP:T2A:Bsd-U6>Scramble_shRNA#1) acquired from Vector Builder (https://en.vectorbuilder.com) containing a gene for blasticidin resistance. Plasmids were expanded in LB medium supplemented with 100µg/mL of Ampicillin; and purified using the QIAprep Spin Miniprep Kit protocol (Qiagen Company, Hilden, Germany, #Cat. 27104), following manufacturer's instructions. To analyze the yield and purity of the plasmids, the NanoDrop Spectrophotometer device (Thermo Scientific, DE, USA) was used. Lentiviral particles were produced by co-transfection of the trans-lentiviral packaging mix with a shRNA transfer vector into HEK 293T packaging cells (OpenBiosystems). For cell infection, viral supernatants were supplemented with 6µg/mL polybrene and incubated with cells for 24 hours. D283 Med transduced cells were selected with blasticidin (10 µg/mL) for 7 days.

Cell cycle analysis

For cell cycle analysis, 17.5x10^{4} (D283 Med *MSI1* knockdown and control shRNA Scramble) cells were plated in 6-well plates and kept in culture for 72h, without treatment. Then, cells were trypsinized and centrifuged at 1,200 rpm/5 min and washed with PBS 1X. Cells were fixed with 70% cold ethanol and incubated at -20^{o} C overnight. Cells were then centrifuged at 800rpm/5 min, washed with PBS 1X, and incubated with 25 µL of RNAse A (10 ng/mL) at 37^{o} C for 30 min. Next, centrifugation step was repeated and cells were stained with 100 µL of PI (50 µg/mL) shortly before acquisition by BD FACS Calibur ™

flow cytometer (BD Biosciences, San Jose, CA, USA). The assay was performed in triplicate. Data were analyzed using FlowJo software.

Cell viability Assay

Cell viability was detected using CellTiter Glo® reagent (Promega) according to the manufacturer's recommendations. Briefly, $6x10^3$ (D283 Med *MSI1* knockdown and control shRNA Scramble) cells were plated in 96-well plates. The cells were treated with cisplatin at different concentrations (3μM, 5μM, 7μM and 10 μM) for 72h, and the results were obtained through SpectraMax® L Microplate Reader device. The assay was performed in triplicate. Furthermore, the concentration of cisplatin that inhibited 50% of cell viability (IC_{50}) was determined by using the CalcuSyn Software (Biosoft, Cambridge, UK).

Apoptosis detection

In total $17.5x10^4$ cells (D283 Med *MSI1* knockdown and control shRNA Scramble) were plated and treatment for 72h with cisplatin at a dose of 4.1 μM. The detection of cell death was performed by labeling apoptotic cells with Annexin V (APC) (BD Biosciences Pharmingen, USA) and Propidium Iodide (PI). Cells were trypsinized and centrifuged at 1,200 rpm for 5 min at 4°C, washed with ice-cold PBS 1X and then resuspended in 200 μL of 1X binding buffer (BD Biosciences Pharmingen, USA) with 5 μL of annexin-V and 50 μL of a solution of PI (50 μM), and incubated for 15 minutes, protected from light, at room temperature. Cells were analyzed by BD FACSCalibur ™ flow cytometer (BD Biosciences, San Jose, CA, USA). The experiments were carried out in triplicate. Data were analyzed using FlowJo 8.7 software.

Statistical analysis

Statistical analysis was performed using the software's (Graph Prism 5.0 GraphPad Software, San Diego, CA USA) and SPSS 15.0 (SPSS Inc. Chicago, USA). Comparisons between two or more groups were carried out using Kruskal-Wallis and One-way-ANOVA, respectively. Receiver operating characteristic (ROC) curves were used to evaluate the discrimination of Grp3/Grp4-MBs from the other molecular subgroups according to *MSI1* expression levels. The accuracy was determined by the area under the curve (AUC). A p-value ≤ 0.05 was considered as statistically significant.

Results

Clinicopathological features of a Brazilian cohort of MBs cases

Clinical data of our cohort of pediatric MB are summarized in Fig. 1A (Fig. 1A). The cohort included 59 primary cases of MBs, in which 15/59 (25.5%) were WNT-MBs, 18/59 (30.5%) SHH-MBs, 9/59 (15.3%) Grp3-MBs and 17/59 (28.7%) Grp4-MBs. Thirty-five children were male and 24 female, and 13/59 (22%) were younger than 3 years at diagnosis. Thirty-eight patients (38/57, 66.6%) achieved gross total and 19

(19/57, 33.4%) subtotal resection. Twenty patients showed metastasis at diagnosis (20/59, 33%). Survival data analysis were performed for all the 59 patients with a median follow-up of 53.9 months (ranging from 3 to 163 months) for progression-free survival (PFS), and 56.4 months (ranging from 3 to 168 months) for overall survival (OS) in 5 years (data not shown).

MSI1 is overexpressed in Grp3/Grp4-MBs subtypes: analysis of an in-house cohort

In order to examine the expression profile of *MSI1* in pediatric MBs, we determined its mRNA expression levels in a Brazilian cohort of 59 MB samples (WNT: n = 15; SHH: n = 18; Grp3: n = 9 and Grp4: n = 17) and five non-neoplastic cerebellums. Furthermore, we explored *MSI1* expression level between different pediatric MB subgroups in a publicly available dataset (GSE85217: WNT n = 51; SHH n = 146; Grp3 n = 131 and Grp4 n = 300). Interestingly, an overexpression of *MSI1* was observed in MBs tissues when compared to normal cerebellum ($P < 0.05$, Fig. 1B). Within MB molecular subtypes, *MSI1* expression was higher in Grp3/Grp-4-MBs ($p < 0.001$ and $p < 0.0001$, respectively) when compared to WNT and SHH-MBs subtypes in our cohort; we have also confirmed the overexpression of *MSI1* in Grp3/Grp4-MBs by analyzing the GSE85217 dataset (Figs. 1B-C).

Once we observed that *MSI1* was overexpressed in both Grp3/Grp4-MBs, we further evaluated its potential significance as a predictive biomarker for MB subgroups. Thus, receiver operating characteristic (ROC) analysis was employed to examine the discrimination accuracy of the *MSI1* as a diagnostic marker for Grp3/Grp4-MBs. As shown in (Fig. 1D), the area under the ROC curve was 0.856 ($p < 0.001$), suggesting a significant high accuracy in discriminating between Grp3/Grp4-MBs from non-Grp3/Grp4-MBs.

To reinforce our initial hypothesis, we evaluated the immunoreactivity of monoclonal anti-MSI1 antibody in formalin-fixed paraffin-embedded samples of pediatric MBs (WNT n = 2; SHH n = 1; Grp3 n = 3 and Grp4 n = 2) by the immunological staining, as summarized in (Table 1). At the protein level, MSI1 staining was strong with score (+) %, percentage of MSI1 positive tumor cells of the +++ (< 50–75%) and ++++ (< 75–100%) in Grp3 (n = 3) and Grp4-MBs (n = 2) tissues (both in nucleus an in the cytoplasm) and low in WNT (n = 2) and SHH (n = 1) tumors with score (+) %, percentage of MSI1 positive tumor cells of the + (< 25%), ++ (< 25–50%), both in nucleus and cytoplasm (Figs. 2A-H and Table 1). Of note, the number of MBs biopsies included in the immunohistochemical staining was limited and insufficient to be correlated to any clinical feature.

Table 1
Immunohistochemical analysis of MSI1 expression in pediatric MBs.

Tumor ID Sample	MB Subtype	Score	Intensity	*MS11*	qRT-PCR (RQ)
1	WNT-MBs	+ +	+	Hipo	4.00
5	SHH-MBs	+ +	+	Hipo	3.30
20	SHH-MBs	+	+	Hipo	0.27
34	Grp3-MBs	+ + +	+ +	Hiper	6.72
35	Grp3-MBs	+ + +	+	Hiper	7.30
42	Grp3-MBs	+ + +	+	Hiper	7.38
43	Grp4-MBs	+ + + +	+ +	Hiper	6.39
58	Grp4-MBs	+ + ++	+ +	Hiper	6.91

Notes: Expression of MSI1 was examined on formalin-fixed, paraffin embedded tissue samples of MBs using immunohistochemistry (IHC). Evaluation of IHC: Score (+) %, percentage of MSI1 positive tumor cells. + (< 25%), ++ (< 25–50%), +++ (< 50–75%) and ++++ (< 75–100%). Intensity of immunostaining (immunoreactivity) in tumor cells: Low (+), Strong (+ +). The hipo or hiperexpression was based in media of expression values of all MBs sample data by qRT-PCR. Value of media expression data is 6.39. RQ = Quantification Relative. Hipoexpressed (Hipo) and Hiperexpressed (Hiper). MB – Medulloblastoma.

MSI1 **is overexpressed in D283 Med: Grp3/Grp4-MBs cell line**

The mRNA and protein levels of *MSI1* were also evaluated by *western blot* and immunofluorescence in two MB cell lines classified as Grp3/Grp4-MBs: D283 Med and USP-13-MED [19, 20]. The D283-Med cells showed an increased expression of *MSI1*, in contrast to USP-13-MED ($p < 0.01$) (Fig. 3A). At protein level, the D283 Med cell line consistently showed higher concentrations of MSI1 when compared to USP-13-MED cells (Figs. 3B-C) by *western blot* analysis. Interestingly, our results of immunofluorescence in the D283 Med cell line showed MSI1 strongly stained in the cytoplasmic and nuclei, while in the USP-13-MED, weak MSI1 staining was observed in the cytoplasm, with dot staining in apical cell extensions of cell-to-cell contact (Figs. 3D-E). According to these findings, we selected the D283-Med cell line to explore the functional roles of *MSI1* into Grp3/Grp4-MBs cells.

Thus, the knockdown of *MSI1* was performed in D283 Med cell line by using lentiviral transduction with two different vectors: shRNA_*MSI1*#1 (constructed to the Exon 4 region) and shRNA_*MSI1*#2 (directed to Exon 8 of *MSI1* gene structure), as well as an empty vector (pure/empty vector - shRNA_Scramble) as a control. The qRT-PCR analysis showed a reduction of approximately 60% in shRNA_*MSI1*#1 and 85% of *MSI1* mRNA levels in shRNA_*MSI1*#2 ($p < 0.001$) cells relative to control (shRNA_Scramble; Fig. 4A). Similarly, the *western blot* analysis of transduced cells revealed a significant reduction of MSI1 protein levels in both shRNA_*MSI1*#1($p < 0.05$) and shRNA_*MSI1*#2 ($p < 0.001$) cells compared with the control

(Figs. 4B-C). Of note, the silencing of *MSI1* was more significant in the cells transduced with the second clone (shRNA_*MSI1*#2).

MSI1 knockdown decreased the number of cells in G2/M phase

MSI1 is known to be associated with cell cycle dysfunction [12]. Thus, we next investigated whether the genetic silencing of *MSI1* would affect cell cycle progression. A higher percentage of D283 Med shRNA_*MSI1*#1 cells were observed in the G0/G1 ($p < 0.0001$) and S phase ($p < 0.001$) compared to control (Figs. 5A-D). However, *MSI1* knockdown decreased the number of cells in G2/M phase in both D283 Med shRNA_*MSI1*#1 and D283 Med shRNA_*MSI1*#2 ($p < 0.01$ and $p < 0.001$, respectively (Fig. 5D).

MSI1 knockdown decreases chemoresistance to cisplatin and increases cell death by apoptosis

Since MBs frequently present resistance to cisplatin treatment [23], we sought to investigate whether the overexpression of *MSI1* is involved in chemoresistance of Grp3/Grp4-MBs cancer cells. To this end, we performed cell viability assays to uncover the effect of the *MSI1* silencing on cellular sensitivity to cisplatin and MB progression *in vitro*. As shown in Fig. 5E, D283 Med shRNA_*MSI1*#1 and D283 Med shRNA_*MSI1*#2 cells were more sensitive to chemotherapy compared to shRNA_Scramble ($p < 0.05$) when treated with different concentrations (3, 5, 7 and 10μM) of cisplatin for 72h. In addition, we observe that knockdown *MSI1* cells were more sensitive to treatment with cisplatin (shRNA_MSI1#1 | IC_{50} 6.6μM and shRNA_MSI1#2 | IC_{50} 4.1μM) when compared to control shRNA_Scramble, IC_{50} 10.98 μM (Fig. 5E and Supplementary Table 01).

To further investigate the mechanism by which *MSI1* knockdown decreases cisplatin resistance, we evaluated the role *MSI1* silencing in triggering cell apoptosis. Annexin V/PI-positive cells were counted as an index of cell death, at the time of 72h treatment, using cisplatin at 4.1 μM (lower dose). As expected, cisplatin treatment induced a significant increase in the apoptosis ratio in the shRNA_Scramble (30%, $p < 0.01$), shRNA_*MSI1*#1 (12%, $p < 0.001$) and shRNA_*MSI1*#2 (63%, $p < 0.001$) compared to untreated cells (Figs. 5F-G). However, this effect was more pronounced in shRNA_*MSI1*#2 (63%, $p < 0.001$) cells, in which we observed an induction around 9 times greater in the rate of apoptosis after cisplatin treatment, while in the shRNA_Scramble this increase was of approximately 5 times (Fig. 5G). Collectively, our findings suggest that *MSI1* knockdown represses D283 Med cells progression whereas sensitizes these cells to cisplatin by enhancing apoptosis of Grp3/Grp4-MBs cancer cells.

Discussion

Currently, the paucity of specific target therapies associated to an increased tumor resistance to current chemotherapeutic regimens are key clinical challenges of Grp3/Grp4-MBs treatment [2, 24]. In this study, we investigated the expression profile and functional roles of *MSI1*, a marker and a regulator of neural stem cells [9, 11–13], in Grp3/Grp4-MBs. *MSI1* is recognized as a key regulator of neural stem cell proliferation and maintenance within the Dentate Gyrus, a part of the hippocampal formation in the

temporal lobe of the brain and the Sub-Ventricular Zone [25]. Of note, any dysregulation of *MSI1* expression is associated with tissue instability and can lead to tumorigenesis [14, 26].

Recent insights into molecular subtype MBs origins hypothesized that during early cerebellar development, the Grp3-MBs arise from progenitor cells of the outer granular layer while Grp4-MBs originate from cells of the upper rhombic lip (uRL) [27, 28]. Herein, we demonstrated that *MSI1* is upregulated in MB tissues compared to normal cerebellum and highlighted its overexpression specifically in Grp3/Grp4-MBs, in contrast to the other MBs subtypes. Thus, we suggest that the overexpression of *MSI1* have a potential role in tumor progression/aggressiveness in this specific setting of MBs.

Consistently with our results, the overexpression of *MSI1* was found in different pediatric brain tumors, such as glioblastomas, gliomas and ependymomas, as well as MBs [15, 16, 29–31]. VO Dat T. *et al.*, (2012) have shown that increased levels *MSI1* in MBs tissues were associated with poor overall and progression-free survival [31]. Due to the limited number of MB biopsies available for immunostaining in our cohort, it was not possible to correlate the levels of MSI1 expression to any clinical feature in Grp3/Grp4-MBs. On the other hand, by using ROC analysis we demonstrated a very high correlation of *MSI1* expression for identifying Grp3/Grp4 cases of MBs, indicating that *MSI1* may be a potential biomarker and could be further explored as a therapeutic target not only for Grp3-MBs, but possibly to Grp4-MBs as well. To our knowledge, the present study is the first to depict *MSI1* a potential as biomarker for Grp3/Grp4-MBs.

Given that cancer is the result of multiple genetic alterations, there are many transcriptional and post-transcriptional mechanisms modulated by RBP's that are involved into key cellular processes, such as cell proliferation and cell fate [12]. However, the role and the underlying molecular mechanisms in which the overexpression of *MSI1* could lead to Grp3/Grp4-MBs oncogenesis remained unexplored. Surprisingly, we observed that the knockdown of *MSI1* promoted cell cycle disruption in the G1/S transition and, consequently, decreased the number of cells in the G2/M phase in Grp3/Grp4-MBs cells. Cell cycle arrest is one important mechanisms by which cancer cells growth may be suppressed [32]. Interestingly, *MSI1* has been proposed to act as a repressor of the translation of mRNAs encoding inhibitors of cell cycle progression [33, 34]. In addition, previous reports have shown that *MSI1* modulates endometrial carcinoma cell cycle progression by $p21^{(WAF1/CIP1)}$ regulation [35]. Also, the knockdown of *MSI1* induced cell cycle arrest at the G1/S phase in hepatoma cells *in vitro* [36], as well as inhibited cell cycle progression by targeting p21 and p27 in human osteosarcoma cells [37]. Recently, a robust study has demonstrated that many of the main target genes of *MSI1* in glioblastoma are involved in cell cycle control, highlighting the cyclin-dependent kinases: *CDK2*, *CDK6*, *CCNA1*, *CCNA2*, as well as p21, and p27 [38].

Another critical aspect of our study was to investigate whether *MSI1* is involved in the progression, drug resistance and induction of programmed cell death in Grp3/Grp4-MBs carcinogenesis. Interestingly, we found that the knockdown of *MSI1* in Grp3/Grp4-MBs cell lines decreased cell survival rate (cell viability) and enhanced cell death by apoptosis in response to cisplatin treatment. Although more studies are

clearly necessary to unravel the mechanistic relationship between these phenomena, in agreement with our findings, it has been reported that *MSI1* is involved in drug resistance of colorectal cancer cells [39], glioblastoma [40] as well as gastric cancer [41].

Likewise, detailed understanding on how *MSI1* may contribute to the processes of drug resistance and cell death in cancer remains elusive to date. Thereby, one of the main goals of this research was to investigate MB cell-line behavior following *MSI1* silencing in association to cisplatin. More recently, new compounds were described to be able to disrupt *MSI1* regulatory functions. These novel *MSI1* inhibitors may be interesting drugs to be tested in animal models, in association to classical chemotherapeutic agents (i.e. cisplatin) for Grp3/4 MB, in order to define if this association may recapitulate *in vivo* tumor arrest and decrease of cisplatin chemoresistance in this setting. Our study has some limitations: the number of patients with MB we were able to include in this study is small. Also, we were able to validate MSI1 expression by IHC only in a few numbers of cases.

Taken together, our results demonstrated that MSI1 is overexpressed in Grp3/Grp4-MBs when compared to non- Grp3/Grp4 tumors. In addition, our findings provide for the first time, experimental evidence indicating that *MSI1* knockdown in association to cisplatin enhances tumor apoptosis by promoting cell cycle disruption and ultimately decreasing cisplatin chemoresistance. These *in-vitro* evidences may support further investigation on the potential role of combining *MSI1* inhibitors to chemotherapy for Grp3/Grp4-MBs.

Declarations

Acknowledgments

We are grateful to Dr. Karina Bezerra Salomão, Me. Veridiana Kiill Suazo, Elizabeth Perna and Deise Chesca for the laboratorial assistance. We also thank Prof. Dr. Oswaldo Keith Okamoto for kindly providing the USP-13-MED cell line for this research, and to Dr Luciano Neder for his diagnostic support on neuropathology. Finally, we would like to thank the patients and families affected by medulloblastomas for their generous contributions to this study.

Author contribution

All authors had full access to all the data in the study and take responsibility for the integrity of the data and the accuracy of the data analysis. Study concept and design: P.F.C designed, conducted, interpreted all experiments, and wrote the manuscript. L.C.V; G.R.S; G.A.V.C; and C.A.P.C wrote and organized the data, created the figures/tables, edited and critically revised the manuscript. FPS performed the histopathologic analysis. R.G.P.Q, S.K.N.M, S.R.B, I.A.C; J.A.Y; C.G.C.J, H.R.M, M.V.S and C.A.S revised the text for important intellectual content. L.G.T and E.T.V designed the study and critically read the manuscript. All authors critically read and approved the final manuscript.

Funding

This study was supported by the São Paulo State Research Foundation (FAPESP), Grant numbers: 2014/20341-0, 2017/26160-5; the Brazilian Research Council (CNPq); the Coordination for the Improvement of Higher Education Personnel (CAPES), Finance Code 001; and the Foundation for Support of Education, Research and Assistance (FAEPA) of the Clinical Hospital of the Ribeirão Preto Medical School - USP, Brazil.

Data availability statement

The data and other items supporting the results of the study will be made available upon reasonable request.

Declarations

Ethics Approval

This study was approved by the HC/FMRP-USP Research Ethics Committee (Approval number: CAAE: 39356920.0.0000.5440) and informed consent was obtained from all patients included.

Consent for publication

Not applicable.

Consent to Participate

Not applicable.

Conflict of interest: The authors declare that they have no competing interests.

References

1. Louis DN, Perry A, Wesseling P, Brat DJ, Cree IA, Figarella-Branger D, Hawkins C, Ng HK, Pfister SM, Reifenberger G, et al. (2021) The 2021 WHO Classification of Tumors of the Central Nervous System: a summary. Neuro Oncol 23: 1231–1251. DOI 10.1093/neuonc/noab106
2. Cavalli FMG, Remke M, Rampasek L, Peacock J, Shih DJH, Luu B, Garzia L, Torchia J, Nor C, Morrissy AS, et al. (2017) Intertumoral Heterogeneity within Medulloblastoma Subgroups. Cancer Cell 31: 737–754.e736. DOI 10.1016/j.ccell.2017.05.005
3. Ray S, Chaturvedi NK, Bhakat KK, Rizzino A, Mahapatra S (2021) Subgroup-Specific Diagnostic, Prognostic, and Predictive Markers Influencing Pediatric Medulloblastoma Treatment. Diagnostics (Basel) 12. DOI 10.3390/diagnostics12010061
4. Northcott PA, Buchhalter I, Morrissy AS, Hovestadt V, Weischenfeldt J, Ehrenberger T, Gröbner S, Segura-Wang M, Zichner T, Rudneva VA, et al. (2017) The whole-genome landscape of medulloblastoma subtypes. Nature 547: 311–317. DOI 10.1038/nature22973

5. Sharma T, Schwalbe EC, Williamson D, Sill M, Hovestadt V, Mynarek M, Rutkowski S, Robinson GW, Gajjar A, Cavalli F, et al. (2019) Second-generation molecular subgrouping of medulloblastoma: an international meta-analysis of Group 3 and Group 4 subtypes. Acta Neuropathol 138: 309–326. DOI 10.1007/s00401-019-02020-0
6. Ramaswamy V, Remke M, Bouffet E, Bailey S, Clifford SC, Doz F, Kool M, Dufour C, Vassal G, Milde T, et al. (2016) Risk stratification of childhood medulloblastoma in the molecular era: the current consensus. Acta Neuropathol 131: 821–831. DOI 10.1007/s00401-016-1569-6
7. Cho YJ, Tsherniak A, Tamayo P, Santagata S, Ligon A, Greulich H, Berhoukim R, Amani V, Goumnerova L, Eberhart CG, et al. (2011) Integrative genomic analysis of medulloblastoma identifies a molecular subgroup that drives poor clinical outcome. J Clin Oncol 29: 1424–1430. DOI 10.1200/JCO.2010.28.5148
8. Nakamura M, Okano H, Blendy JA, Montell C (1994) Musashi, a neural RNA-binding protein required for Drosophila adult external sensory organ development. Neuron 13: 67–81. DOI 10.1016/0896–6273(94)90460-x
9. Kaneko Y, Sakakibara S, Imai T, Suzuki A, Nakamura Y, Sawamoto K, Ogawa Y, Toyama Y, Miyata T, Okano H (2000) Musashi1: an evolutionally conserved marker for CNS progenitor cells including neural stem cells. Dev Neurosci 22: 139–153. DOI 10.1159/000017435
10. Sakakibara S, Imai T, Hamaguchi K, Okabe M, Aruga J, Nakajima K, Yasutomi D, Nagata T, Kurihara Y, Uesugi S, et al. (1996) Mouse-Musashi-1, a neural RNA-binding protein highly enriched in the mammalian CNS stem cell. Dev Biol 176: 230–242. DOI 10.1006/dbio.1996.0130
11. Sakakibara S, Nakamura Y, Satoh H, Okano H (2001) Rna-binding protein Musashi2: developmentally regulated expression in neural precursor cells and subpopulations of neurons in mammalian CNS. J Neurosci 21: 8091–8107
12. Kudinov AE, Karanicolas J, Golemis EA, Boumber Y (2017) Musashi RNA-Binding Proteins as Cancer Drivers and Novel Therapeutic Targets. Clin Cancer Res 23: 2143–2153. DOI 10.1158/1078 – 0432.CCR-16-2728
13. Okano H, Imai T, Okabe M (2002) Musashi: a translational regulator of cell fate. J Cell Sci 115: 1355–1359
14. das Chagas PF, Baroni M, Brassesco MS, Tone LG (2020) Interplay between the RNA binding-protein Musashi and developmental signaling pathways. J Gene Med 22: e3136. DOI 10.1002/jgm.3136
15. Dahlrot RH, Hansen S, Herrstedt J, Schrøder HD, Hjelmborg J, Kristensen BW (2013) Prognostic value of Musashi-1 in gliomas. J Neurooncol 115: 453–461. DOI 10.1007/s11060-013-1246-8
16. Lin JC, Tsai JT, Chao TY, Ma HI, Liu WH (2019) Musashi-1 Enhances Glioblastoma Migration by Promoting ICAM1 Translation. Neoplasia 21: 459–468. DOI 10.1016/j.neo.2019.02.006
17. Ma YH, Mentlein R, Knerlich F, Kruse ML, Mehdorn HM, Held-Feindt J (2008) Expression of stem cell markers in human astrocytomas of different WHO grades. J Neurooncol 86: 31–45. DOI 10.1007/s11060-007-9439-7

18. Cruzeiro GAV, Salomão KB, de Biagi CAO, Baumgartner M, Sturm D, Lira RCP, de Almeida Magalhães T, Baroni Milan M, da Silva Silveira V, Saggioro FP, et al. (2019) A simplified approach using Taqman low-density array for medulloblastoma subgrouping. Acta Neuropathol Commun 7: 33. DOI 10.1186/s40478-019-0681-y
19. Friedman HS, Burger PC, Bigner SH, Trojanowski JQ, Wikstrand CJ, Halperin EC, Bigner DD (1985) Establishment and characterization of the human medulloblastoma cell line and transplantable xenograft D283 Med. J Neuropathol Exp Neurol 44: 592–605. DOI 10.1097/00005072-198511000-00005
20. Silva PB, Rodini CO, Kaid C, Nakahata AM, Pereira MC, Matushita H, Costa SS, Okamoto OK (2016) Establishment of a novel human medulloblastoma cell line characterized by highly aggressive stem-like cells. Cytotechnology 68: 1545–1560. DOI 10.1007/s10616-015-9914-5
21. Schmittgen TD, Livak KJ (2008) Analyzing real-time PCR data by the comparative C(T) method. Nat Protoc 3: 1101–1108. DOI 10.1038/nprot.2008.73
22. Lovell MA, Markesbery WR (2005) Ectopic expression of Musashi-1 in Alzheimer disease and Pick disease. J Neuropathol Exp Neurol 64: 675–680. DOI 10.1097/01.jnen.0000173891.17176.5b
23. Gilbertson RJ (2004) Medulloblastoma: signalling a change in treatment. Lancet Oncol 5: 209–218. DOI 10.1016/S1470-2045(04)01424-X
24. Parsons DW, Li M, Zhang X, Jones S, Leary RJ, Lin JC, Boca SM, Carter H, Samayoa J, Bettegowda C, et al. (2011) The genetic landscape of the childhood cancer medulloblastoma. Science 331: 435–439. DOI 10.1126/science.1198056
25. Sakakibara S, Okano H (1997) Expression of neural RNA-binding proteins in the postnatal CNS: implications of their roles in neuronal and glial cell development. J Neurosci 17: 8300–8312
26. Fox RG, Park FD, Koechlein CS, Kritzik M, Reya T (2015) Musashi signaling in stem cells and cancer. Annu Rev Cell Dev Biol 31: 249–267. DOI 10.1146/annurev-cellbio-100814-125446
27. Marino S (2005) Medulloblastoma: developmental mechanisms out of control. Trends Mol Med 11: 17–22. DOI 10.1016/j.molmed.2004.11.008
28. Lin CY, Erkek S, Tong Y, Yin L, Federation AJ, Zapatka M, Haldipur P, Kawauchi D, Risch T, Warnatz HJ, et al. (2016) Active medulloblastoma enhancers reveal subgroup-specific cellular origins. Nature 530: 57–62. DOI 10.1038/nature16546
29. Nakano A, Kanemura Y, Mori K, Kodama E, Yamamoto A, Sakamoto H, Nakamura Y, Okano H, Yamasaki M, Arita N (2007) Expression of the Neural RNA-binding protein Musashi1 in pediatric brain tumors. Pediatr Neurosurg 43: 279–284. DOI 10.1159/000103307
30. Toda M, Iizuka Y, Yu W, Imai T, Ikeda E, Yoshida K, Kawase T, Kawakami Y, Okano H, Uyemura K (2001) Expression of the neural RNA-binding protein Musashi1 in human gliomas. Glia 34: 1–7. DOI 10.1002/glia.1034
31. Vo DT, Subramaniam D, Remke M, Burton TL, Uren PJ, Gelfond JA, de Sousa Abreu R, Burns SC, Qiao M, Suresh U, et al. (2012) The RNA-binding protein Musashi1 affects medulloblastoma growth via a

network of cancer-related genes and is an indicator of poor prognosis. Am J Pathol 181: 1762–1772. DOI 10.1016/j.ajpath.2012.07.031

32. Williams GH, Stoeber K (2012) The cell cycle and cancer. J Pathol 226: 352–364. DOI 10.1002/path.3022
33. Okano H, Kawahara H, Toriya M, Nakao K, Shibata S, Imai T (2005) Function of RNA-binding protein Musashi-1 in stem cells. Exp Cell Res 306: 349–356. DOI 10.1016/j.yexcr.2005.02.021
34. MacNicol MC, Cragle CE, MacNicol AM (2011) Context-dependent regulation of Musashi-mediated mRNA translation and cell cycle regulation. Cell Cycle 10: 39–44. DOI 10.4161/cc.10.1.14388
35. Götte M, Greve B, Kelsch R, Müller-Uthoff H, Weiss K, Kharabi Masouleh B, Sibrowski W, Kiesel L, Buchweitz O (2011) The adult stem cell marker Musashi-1 modulates endometrial carcinoma cell cycle progression and apoptosis via Notch-1 and p21WAF1/CIP1. Int J Cancer 129: 2042–2049. DOI 10.1002/ijc.25856
36. Li J, Yan K, Yang Y, Li H, Wang Z, Xu X (2019) [Musashi-1 positively regulates growth and proliferation of hepatoma cells. Nan Fang Yi Ke Da Xue Xue Bao 39: 1436–1442. DOI 10.12122/j.issn.1673-4254.2019.12.07
37. Niu J, Zhao X, Liu Q, Yang J (2017) Knockdown of MSI1 inhibited the cell proliferation of human osteosarcoma cells by targeting p21 and p27. Oncol Lett 14: 5271–5278. DOI 10.3892/ol.2017.6870
38. Baroni M, Yi C, Choudhary S, Lei X, Kosti A, Grieshober D, Velasco M, Qiao M, Burns SS, Araujo PR, et al. (2021) Musashi1 Contribution to Glioblastoma Development via Regulation of a Network of DNA Replication, Cell Cycle and Division Genes. Cancers (Basel) 13. DOI 10.3390/cancers13071494
39. Chiou GY, Yang TW, Huang CC, Tang CY, Yen JY, Tsai MC, Chen HY, Fadhilah N, Lin CC, Jong YJ (2017) Musashi-1 promotes a cancer stem cell lineage and chemoresistance in colorectal cancer cells. Sci Rep 7: 2172. DOI 10.1038/s41598-017-02057-9
40. Chen HY, Lin LT, Wang ML, Tsai KL, Huang PI, Yang YP, Lee YY, Chen YW, Lo WL, Lan YT, et al. (2018) Musashi-1 promotes chemoresistant granule formation by PKR/eIF2α signalling cascade in refractory glioblastoma. Biochim Biophys Acta Mol Basis Dis 1864: 1850–1861. DOI 10.1016/j.bbadis.2018.02.017
41. Xu M, Gong A, Yang H, George SK, Jiao Z, Huang H, Jiang X, Zhang Y (2015) Sonic hedgehog-glioma associated oncogene homolog 1 signaling enhances drug resistance in CD44(+)/Musashi-1(+) gastric cancer stem cells. Cancer Lett 369: 124–133. DOI 10.1016/j.canlet.2015.08.005

Figures

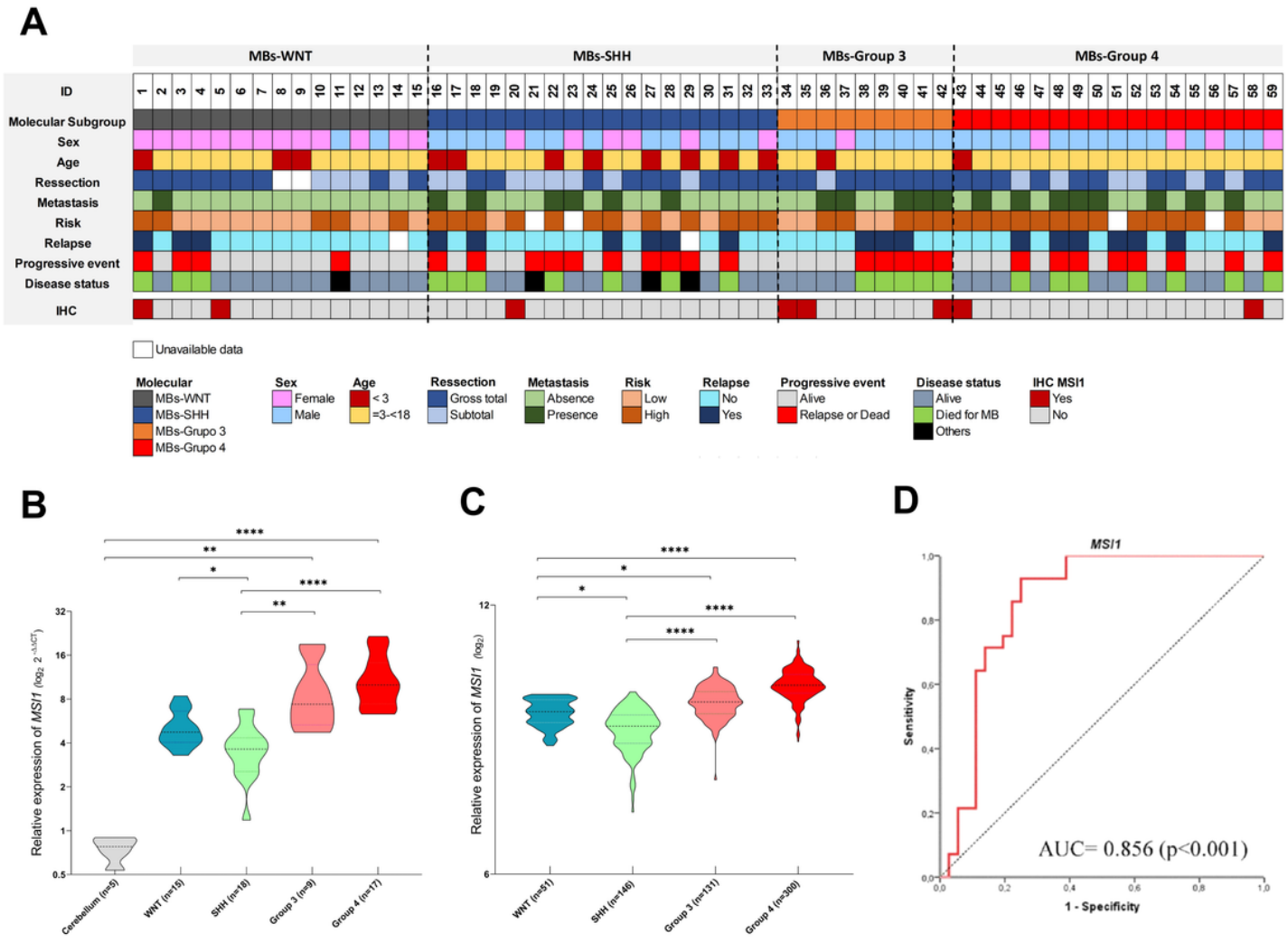

Figure 1

Clinicopathological features and *MSI1* expression overview in a Brazilian cohort of MBs. (A) Summary of clinical features and molecular characteristics of tumor samples from 59 pediatric patients: Molecular classification (WNT-MBs; SHH-MBs; Grp3-MBs and Grp4-MBs); gender (female or male); Age at diagnosis (below or above 3 years); tumor resection (Gross total resection GTR or subtotal resection STR); tumor metastasis (Absent or Present); risk stratification (Average or High); tumor relapse (yes or no); Patient status and outcome (alive or tumor relapse/death); Disease status (alive; death related to MB or others). Samples used for the evaluation of MSI1 expression by IHC (immunohistochemistry). **(B)** Relative gene expression of *MSI1* in an in-house cohort of MBs and normal cerebellum (Cerebellum n-5; WNT n=15; SHH n=18; Grp3 n=9 and Grp4 n=17) by qRT-PCR. ANOVA were conducted using the Tukey multiple comparisons post-test to assess the statistical significance between groups. *indicates (p<0.01), ** (p<0.001) and ****(p<0.0001). **(C)** Evaluation of *MSI1* expression profiling in pediatric MBs using data expression of dataset GSE85217 (MBs samples: WNT n=51; SHH n=146; Grp3 n=131 and Grp4 n=300). **(D)** Receiver operating characteristic (ROC) analysis of the diagnostic value of *MSI1* in distinguishing Grp3/Grp4-MBs and WNT/SHH-MBs based on data expression of an in-house cohort.

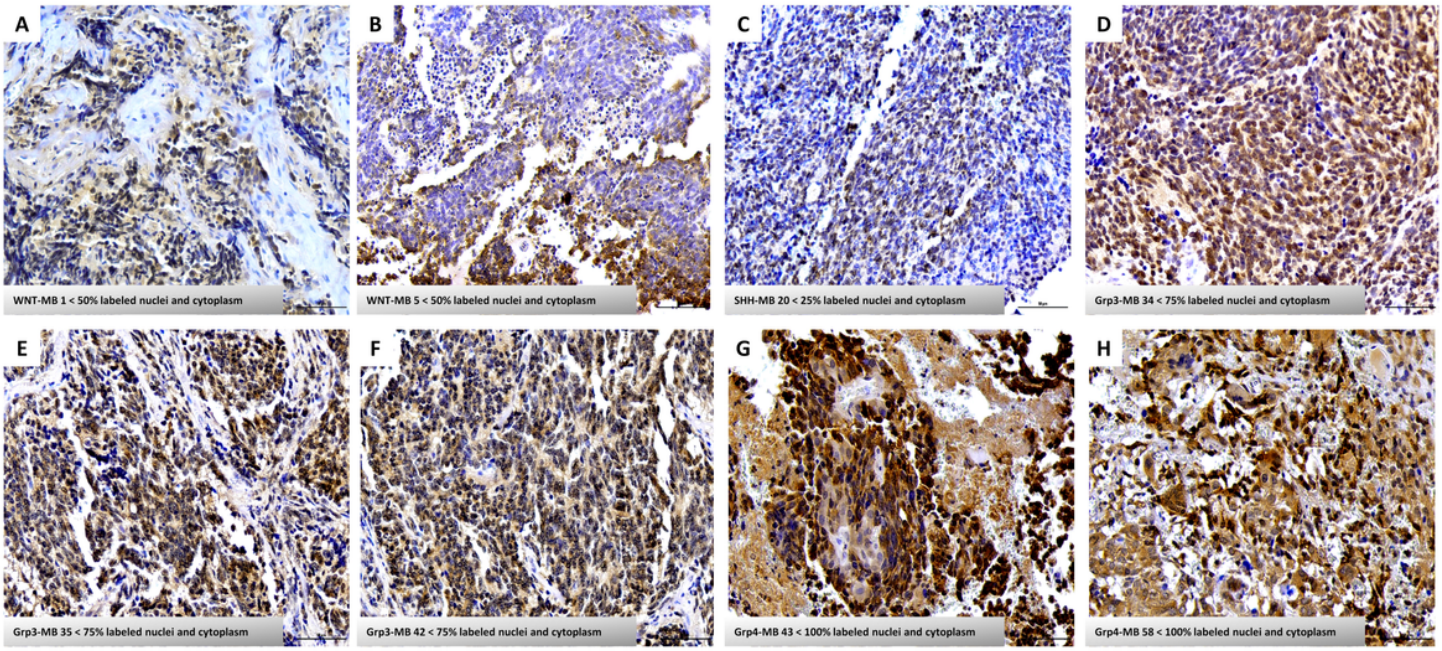

Figure 2

MSI1 Immunostaining and prediction. **(A-H)** Representative microscopic images depicting the MSI1 staining (brown) and showing positivity levels in MBs tissues by IHQ. WNT/SHH-MBs subtypes exhibited the low immunostaining to MSI1 (<50%); in contrast, Grp3/Grp4-MBs demonstrate high immunostaining to MSI1 (<100%). Both of subtypes showed nucleus and cytoplasm labeled. Scale bar, 50 μm. Original magnification ^{x}20.

Figure 3

Characterization of *MSI1* expression in Grp3/Grp4-MBs cell line models: (A) Relative expression of *MSI1* by RT-qPCR in D283 Med and USP-13-MED cell lines. The graph shows the mean ± standard deviation of three independent experiments (*p<0.01). (**B)** Relative MSI1 protein quantification. (**C)** Representative image of protein profile of MSI1 by *Western blot* in pediatric MB cell lines D283 Med and USP-13-MED. GAPDH protein was used as an endogenous control. The relative quantification of protein expression was determined by ImageJ software. Representative photomicrographs of the immunofluorescence technique: Fluorescence intensity and location of MSI1 (magenta). (**D)** D283 Med – strong intensity for the nucleus and cytoplasm; (**e)** USP-13-MED – medium intensity for the cytoplasm and weak for the nucleus. Notes: Expression of MSI1 in cell lines was examined using indirect immunofluorescence method. Analysis by confocal laser scanning microscopy.

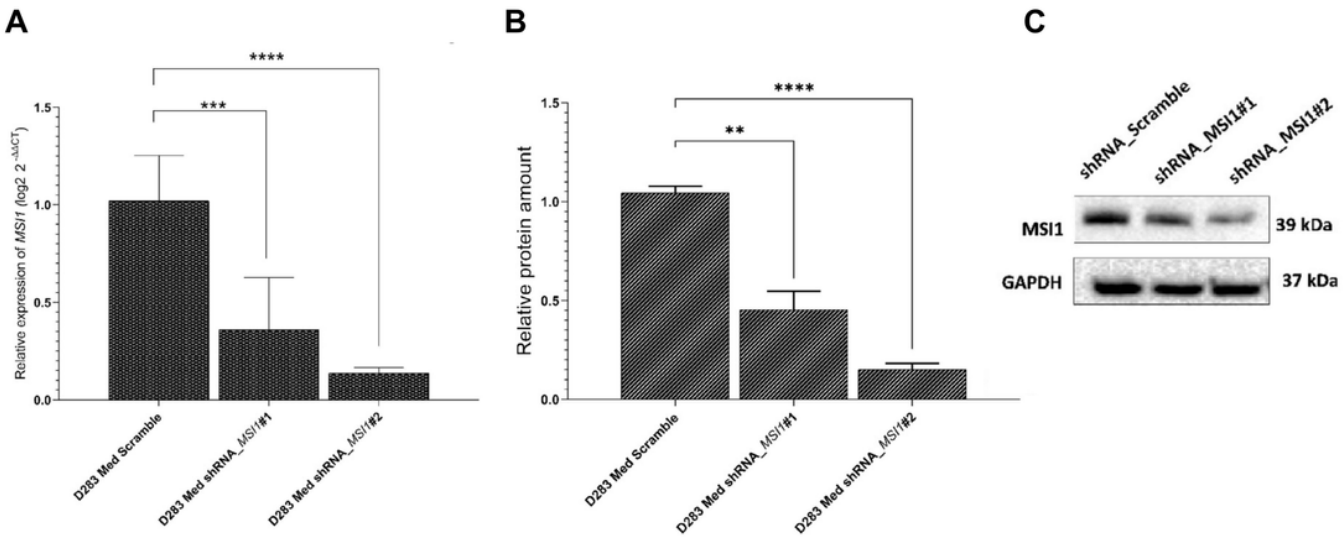

Figure 4

***MSI1* knockdown**: (**A**) Relative expression of *MSI1* by RT-qPCR (**B**-**C**) Protein quantification of *MSI1* by *Western blot* in D283 Med cell lines after gene modulation. Relative quantification of protein expression was performed using ImageJ software. GAPDH protein was used as an endogenous control. All graphs show mean ± standard deviation (SD) of three independent experiments. **p<0.05; ***p<0.01 and ****p<0.001, compared to control (Scramble).

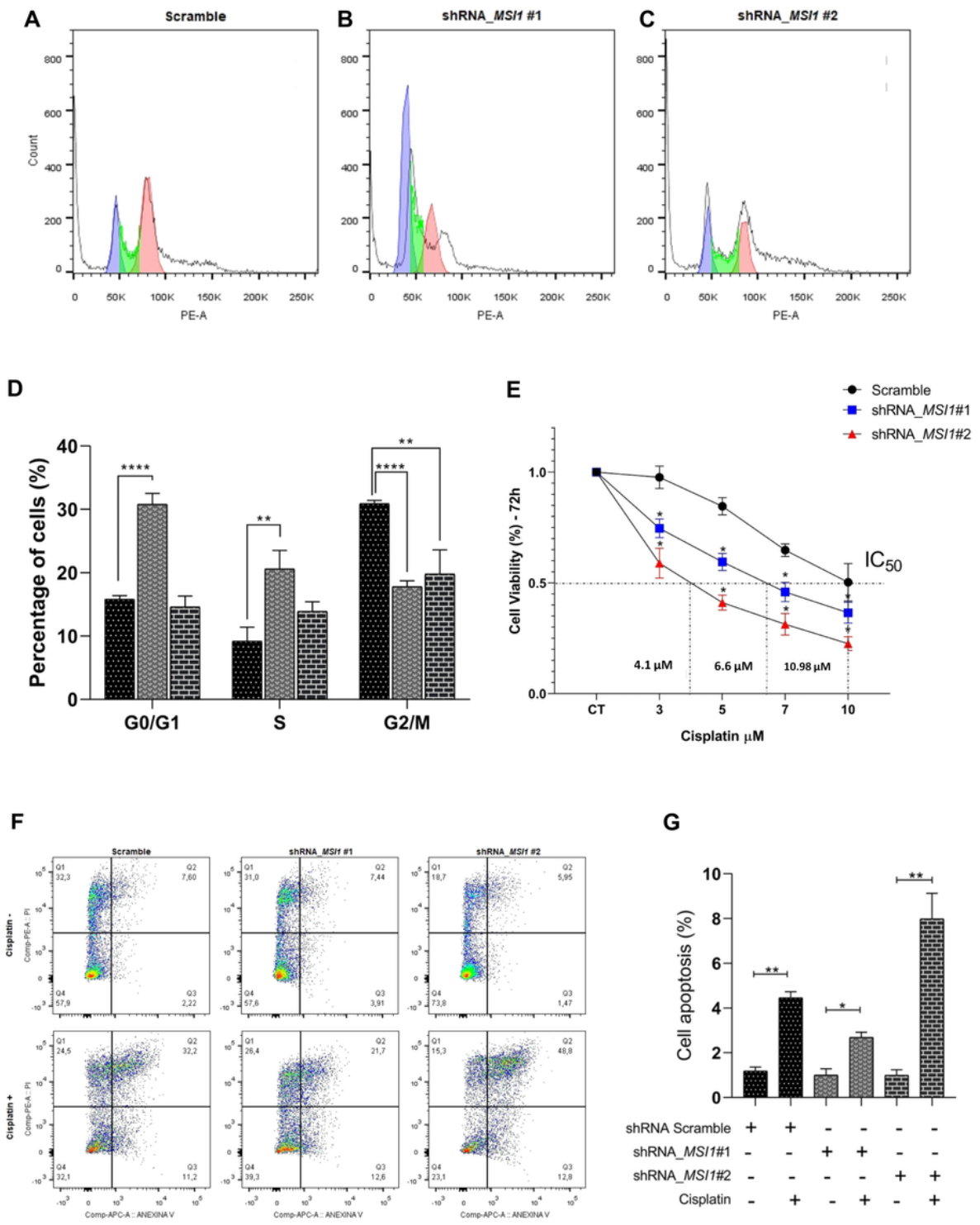

Figure 5

Impact of *MSI1* knockdown in D283 Med (Grp3/Grp4-MBs) cells. **(A-C)** The cell cycle histograms. **(D)** The knockdown of *MSI1* in the D283 Med shRNa_*MSI1*#1 and D283 Med shRNA_*MSI1*#2 cells decreased G2/M phase when compared to shRNA_Scramble. **(E)** Cell viability was assessed by Cell Titer assay. Reduction of cell proliferation of D283 Med shRNa_*MSI1*#1 and D283 Med shRNA_*MSI1*#2 after cisplatin treatment (3, 5, 7 and 10 µM) for 72 hours compared to shRNA_Scramble. The IC_{50} values of cisplatin

treatment in D283 Med shRNa_*MSI1*#1, D283 Med shRNA_*MSI1*#2 and shRNA_Scramble are 4.1 µM, 6.6 µM and 10.98 µM, respectively. **(F-G)** knockdown of *MSI1* associated with cisplatin treatment in D283 Med cells increased cell apoptosis. Apoptosis was detected by flow cytometry after Annexin and propidium iodide staining. Two-Way ANOVA Test. The graphs show the mean ± standard deviation of three independent experiments. *p<0.05; **p<0.01 and ****p<0.001 compared to control (shRNA_Scramble).

Supplementary Files

This is a list of supplementary files associated with this preprint. Click to download.

- SupplementaryTable01.docx